

BAYESIAN CLASSIFICATION, ANOMALY DETECTION, AND SURVIVAL ANALYSIS USING NETWORK INPUTS WITH APPLICATION TO THE MICROBIOME

BY NATHANIEL JOSEPHS¹, LIZHEN LIN², STEVEN ROSENBERG¹
AND ERIC D. KOLACZYK¹

¹*Department of Mathematics and Statistics, Boston University*

²*Department of Applied and Computational Mathematics and Statistics, The University of Notre Dame*

While the study of a single network is well-established, technological advances now allow for the collection of multiple networks with relative ease. Increasingly, anywhere from several to thousands of networks can be created from brain imaging, gene co-expression data, or microbiome measurements. And these networks, in turn, are being looked to as potentially powerful features to be used in modeling. However, with networks being non-Euclidean in nature, how best to incorporate networks into standard modeling tasks is not obvious. In this paper, we propose a Bayesian modeling framework that provides a unified approach to binary classification, anomaly detection, and survival analysis with network inputs. Our methodology exploits the theory of Gaussian processes and naturally requires the use of a kernel, which we obtain by modifying the well-known Hamming distance. Moreover, kernels provide a principled way to integrate data of mixed types. We motivate and demonstrate the whole of our methodology in the area of microbiome research, where network analysis is emerging as the standard approach for capturing the interconnectedness of microbial taxa across both time and space.

1. Introduction. Suppose we have data $(X_1, Y_1), \dots, (X_N, Y_N)$. One of the last topics in Statistics 101 is linear regression in the case that Y is continuous. In later courses, we learn about classification if Y is binary, then maybe survival analysis if Y is a time-to-event. If there are dependencies in the data, we learn how to model time-series or random effects. In all these cases, we typically have $X \in \mathbb{R}^p$. And we spend a lot of time thinking about when $p > N$. But what if X is a network? Or a combination of networks and real numbers? While years ago this question would have seemed like a mathematical exercise, technological advances are making this question a reality.

One such area that has received much attention in recent years is the microbiome, with nearly \$2 billion spent on research in the past decade according to [Proctor \(2019\)](#). Emerging from this research is the use of network analyses to disentangle the complex interconnectedness of taxa within a microbiome. A recent review of the current state of applying network analyses to microbiome data is given by [Layeghifard, Hwang and Guttman \(2017\)](#). The authors cover various methods of network construction, as well as highlight ecological network analyses such as identifying biologically important clusters, detecting keystone species, and capturing microbiome dynamics. However, they also state that “most current work concentrates on snapshots of activity in a few selected environments and in an abstract space.”

Moving away from this static view of the microbiome, [Faust et al. \(2018\)](#) create individual microbial networks from high-resolution time-series data. However, this data is only for two individuals, which underscores the current paradigm: most microbiome studies either have many subjects but few time points or many time points for only a few subjects.

Keywords and phrases: Multiple Networks, Gaussian Processes, Graph Kernel, Hamming Distance, Preterm Delivery

One dataset that is uniquely interesting due to its balance of granularity and sample size is from [DiGiulio et al. \(2015\)](#). The authors tracked the microbiomes of 40 women over the course of their pregnancies by collecting over 3400 samples from the vagina, distal gut, saliva, and tooth/gum areas. This effort resulted in a rich dataset that revealed the presence of over 1200 different taxa. The authors aim was to identify microbial taxa associated with a higher risk of preterm delivery, which occurred in 15 of the 40 women in the study. We summarize the lengths of gestation in Figure 1.

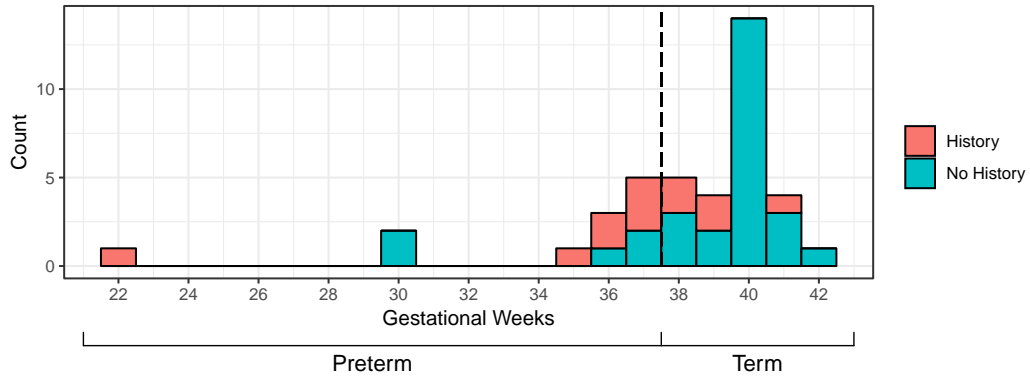


FIG 1. Histogram of lengths of gestational periods in weeks. The dashed line separates the classes of term, which is delivery after 37 weeks, from preterm. Red and blue represent women with and without a history of preterm delivery, respectively.

Preterm delivery is a global health problem and hence an important area of research. A better understanding of the relationship between preterm delivery and microbiome measurements that are sufficiently easy to obtain could help to inform routine prenatal care decisions, as well as to provide important controls in studies of pregnant women. In their analysis, [DiGiulio et al. \(2015\)](#) successfully identified several taxa whose dynamics throughout the gestational period were significantly related to a higher risk of preterm delivery. Additionally, these authors looked at the interconnectedness of taxa at the level of taxonomic communities. Ultimately, corresponding network summary values were used as descriptors for linear mixed-effect models. The resulting findings suggest that individual microbiomes – as captured through network-based representations – can be important descriptors for various pregnancy outcomes.

Examples of such networks are shown in Figure 2. In [DiGiulio et al. \(2015\)](#) and other microbiome analyses, the strategy has been to identify and extract certain potentially relevant aspects of the topology of these networks for downstream analysis. However, it is clear from these visualizations that microbiome networks possess a rich topology, and that they can exhibit important topological differences across, for example, patient subgroups. Without knowing precisely which aspects of network topology might be most relevant to a given study, it is increasingly desirable to have statistical methods that allow researchers to incorporate the *entire* network, rather than only numerical summaries.

Anticipating this need, we propose here a unified methodology for analyzing datasets for a number of standard purposes – namely, classification, anomaly detection, and survival analysis – using whole-network inputs. A schematic diagram is given in Figure 3. In the context of using individual microbiome networks for clinical purposes, and the dataset described above,

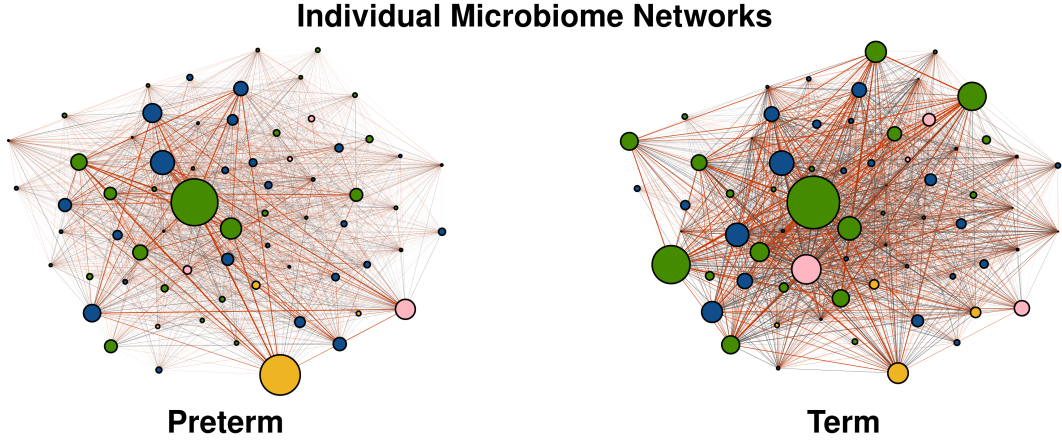


FIG 2. Examples of individual microbiome networks. Nodes represent different species of bacteria. Each node is colored by primary area of collection and the size is proportional to the mean count of that species over all of the individual's samples. Edges correspond to association between the species with the edge thickness corresponding to the strength of association. Black edges are negative associations and red are positive. Details of the network constructions are outlined in Section 5.2.

our methodological contribution allows researchers to address the following important questions. First, can we identify women at a high risk of preterm delivery? Second, can we do so even if this event is rare in the dataset? Finally, can we understand gestational length as a time-to-event? The ability to better answer these questions promises to improve the personalization of prenatal care. More generally, we expect our contributions here to advance the use of networks to analyze the microbiome, both now and in the future. Specifically, our Bayesian approach can help mitigate the challenges of small sample size (McNeish (2016)), which typifies most current microbiome experiments, and at the same time our approach scales to the expected paradigm shift toward microbiome studies that sample with higher resolution for many individuals.

1.1. *Background.* We briefly review relevant network and Gaussian process (GP) concepts. For more thorough reviews of the statistical analysis of network data and the use of GPs in machine learning, see Kolaczyk and Csárdi (2014) and Rasmussen and Williams (2005), respectively.

A *network* or *graph* G is an ordered pair (V, E) consisting of a set of nodes or vertices, V , and edges, E , where $e \in E(G)$ is a pair of nodes $(v_1, v_2) \in V(G) \times V(G)$. Throughout, we work with *undirected* and *simple* networks, meaning that there is no directional component to our edges and no self loops. Furthermore, we will work with networks of the same *order*, i.e. for networks G_1, \dots, G_N , we have $|V_1| = |V_2| = \dots = |V_N| = n$. For computations and analyses, graphs are represented through matrices. The *adjacency matrix* of a graph G with nodes $V(G) = (v_1, \dots, v_n)$ is an $n \times n$ matrix A with

$$A_{ij} = \begin{cases} 1 & \text{if } v_i \text{ adjacent to } v_j \\ 0 & \text{otherwise} \end{cases}.$$

For *weighted networks*, which are triples $G = (V, E, W)$, the corresponding *weighted adjacency matrix* is defined similarly:

$$A_{ij} = \begin{cases} w_{ij} & \text{if } \{i, j\} \in E \\ 0 & \text{otherwise} \end{cases}.$$

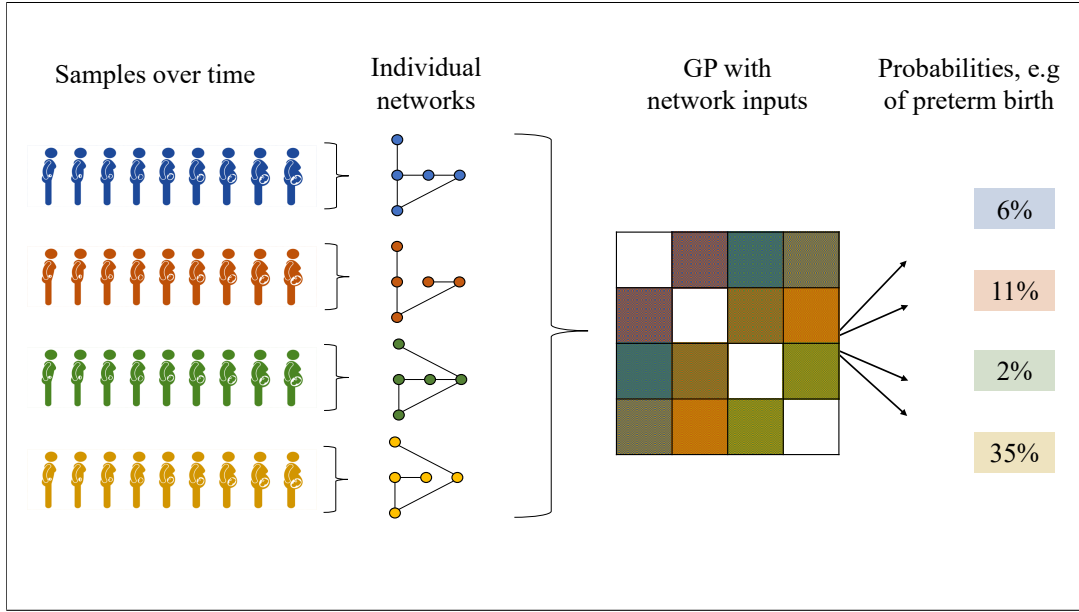


FIG 3. Schematic diagram of study design, network construction, and probabilistic modeling with network inputs.

A *Gaussian process* is a collection of random variables of which any finite subset is jointly Gaussian. We write

$$f(x) \sim \mathcal{GP}(m(x), k(x, x')) ,$$

where $m(x) = \mathbb{E}[f(x)]$ and $k(x, x') = \mathbb{E}[(f(x) - m(x))(f(x') - m(x'))]$. The use of GPs for machine learning is a Bayesian nonparametric kernel method, where latent functions are given GP priors. Typically, GP priors are taken to be mean zero and all relevant information is encoded in the covariance function k . For that reason, learning with GPs is equivalent to learning the covariance hyperparameters. The most widely used covariance function is the squared-exponential,

$$(1) \quad k(x_i, x_j) = \sigma^2 \exp\left(-\frac{|x_i - x_j|^2}{2\ell^2}\right) ,$$

where σ^2 and ℓ are the *signal variance* and *length-scale* parameters. For any proper covariance function k , the resulting Gram matrix K with $K_{ij} = k(x_i, x_j)$ is called a *kernel*.

We expect collections of networks to often be accompanied by other data, and kernels provide a principled way to combine data of mixed types, sometimes referred to as multimodal data. This follows from the fact that kernels are closed under addition and multiplication. If we have multiple networks per individual, continuous or binary variables, or any other data that can be encoded in a squared-exponential kernel, then we can combine them additively, which has two nice properties. First, by using one overall signal variance, we retain conjugacy in our sampler. Second, each length-scale parameter can be thought of as automatically performing relevance detection of the variables.

As mentioned before, learning with kernels is tantamount to learning the kernel hyperparameters and this challenge is exacerbated with many variables, since each kernel will have its own length-scale parameter. Fortunately, the Bayesian framework is perfectly suited to this problem, as one of the main features of a Bayesian approach is the use of hierarchical models. That is, we will put hyperpriors over each hyperparameter in order to fully explore the

kernel hyperparameter space via the posterior. While certain techniques like grid searching or maximizing the marginal likelihood offer fast approximations in low-dimensions, they are inexact, which is compounded in high-dimensional settings for which their speed is negated anyway. For this reason, a fully Bayesian approach is the most appropriate way to learn the kernels. In addition, the Bayesian framework is probabilistic, which lends itself naturally to uncertainty quantification. In our context, that will not only mean uncertainty quantification of our posterior predictions, but an immediate extension to anomaly detection. Finally, the Bayesian framework allows for prior specification, which is always relevant for applied problems when working with domain experts. For example, clinicians can inform priors for the baseline hazard function in a survival analysis.

1.2. Related Work. There is a large literature on graph kernels beginning with [Kondor and Lafferty \(2002\)](#), who propose diffusion kernels for graphs and suggest that they could be used in conjunction with GPs. Shortly thereafter, [Gärtner, Driessens and Ramon \(2003\)](#) propose the random walk graph kernel, which the authors use to perform a variant of GP regression. To the best of our knowledge, this is the only explicit use of GPs with graphs. [Kashima and Inokuchi \(2002\)](#) apply similar graph kernels for classification, but not using a GP framework. Since then, there have been many other graph kernels proposed. For a survey on graph kernels, see [Vishwanathan et al. \(2010\)](#); [Kriege, Johansson and Morris \(2020\)](#); [Nikolentzos, Siglidis and Vazirgiannis \(2019\)](#).

Regarding the use of network inputs, a Bayesian approach seems not to have been applied to classification problems. However, kernel support vector machines (SVMs) have been a popular tool for classification with network inputs, and extensions exist to one-class classification and survival analysis. In particular, graph data has been used with SVMs to perform classification of protein function prediction ([Borgwardt et al. \(2005\)](#)), chemical informatics ([Ralaivola et al. \(2005\)](#)), and disease ([Rudd \(2018\)](#)), as well as one-class classification for media data ([Mygdalis et al. \(2016\)](#)). In Section 2.1, we will show the connection between the kernel SVM solution and our GP solution.

Alternatively, [Relión et al. \(2019\)](#) provide a frequentist approach to classification with network inputs. Interestingly, in comparing their method to others, the authors say that “kernel methods were no better than random guessing.” They also claim that “kernel methods [are] unsuitable for large scale networks.” Throughout, we demonstrate that, in fact, our method is highly scalable to large networks and outperforms the authors’ method on their classification task.

Elsewhere, [Zhang et al. \(2013\)](#) introduce Net-Cox for survival analysis with network inputs, which is a network-constrained Cox regression using the graph Laplacian as a penalty. The authors note that “surprisingly, network-based survival analysis has not received enough attention.” We will discuss the benefits of our survival analysis methodology, which is not a proportional hazards model, in Section 2.3.

Finally, there is a growing body of work on statistical analysis of multiple networks in general. For example, Jain and colleagues have a number of contributions, summarized, for example, in [Jain \(2016\)](#), where they propose the use of linear classifiers in graph space. While our work also has some geometrical underpinnings, it is nevertheless distinct. Similarly, there is various work on network-based extensions of averages ([Ginestet et al. \(2017\)](#); [Durante, Dunson and Vogelstein \(2017\)](#); [Tang et al. \(2018\)](#); [Kolaczyk et al. \(2020\)](#)), regression ([Cornea et al. \(2017\)](#)), and PCA ([Dai et al. \(2018\)](#)), to name a few. Again, however, our work is distinct.

1.3. Paper Outline. The remainder of the paper is organized as follows. In Section 2, we set up our models for binary classification, anomaly detection, and survival analysis. We

discuss implementation and theoretical results for our models in Section 3 and Section 4, respectively. We return to the microbiome dataset in Section 5, where we present the results of our analyses along with simulation results. Finally, we conclude in Section 6 with a discussion of future directions for this work.

2. Models.

2.1. *Binary Classification.* Suppose we have data $(G_1, Y_1), \dots, (G_N, Y_N)$, where

$$G \in \mathcal{G} := \{(\text{labeled}) \text{ weighted networks of order } n\}$$

and Y is binary. We are interested in learning the classification map $\pi(G) := p(y = 1 | G)$. To do this, we will directly model $\pi(G)$ using Bayesian inference. In particular, we equip $\pi(G)$ with a prior that is a deterministic transformation of a GP on \mathcal{G} . That is, $\pi(G) = H(f(G))$ for some link function H and latent function $f := f(G)$. We then place a GP prior on \mathcal{G} with kernel K over f . Throughout, we work with the logistic link, $\sigma(z) = 1/(1 + \exp(-z))$, and kernel given by

$$(2) \quad K_{ij} = \sigma^2 \exp \left(-\ell \cdot d_{\text{Ham}}(G_i, G_j) \right) ,$$

where d_{Ham} is defined in Section 4.1. In addition to the GP prior on our latent function f , we place inverse-gamma priors on the kernel hyperparameters. Regarding our likelihood, note that if we take $Y \in \{\pm 1\}$, then we can write

$$p(y | f) = \sigma(f \cdot y) ,$$

as $\sigma(-z) = 1 - \sigma(z)$ and $p(y = 1 | G) + p(y = -1 | G) = 1$. Below, we summarize our model, including the posterior from which we will make inference on $\pi(G)$:

$$\begin{aligned} \text{likelihood: } & p(y | f) = \prod_{i=1}^N \sigma(f_i y_i) ; \\ \text{prior: } & p(f | G, \sigma^2, \ell) \propto e^{-\frac{1}{2} f^T K^{-1} f} , \\ & p(\sigma^2) \propto (\sigma^2)^{-\alpha_1 - 1} e^{-\frac{\beta_1}{\sigma^2}} , \\ & p(\ell) \propto \ell^{-\alpha_2 - 1} e^{-\frac{\beta_2}{\ell}} ; \\ \text{posterior: } & p(f | G, y, \sigma^2, \ell) \propto p(y | f) p(f | G, \sigma^2, \ell) p(\sigma^2) p(\ell) . \end{aligned}$$

For a new network \tilde{G} , the posterior predictive distributions are

$$\begin{aligned} p(\tilde{f} | G, y, \tilde{G}) &\propto p(\tilde{f} | G, \tilde{G}, f) p(f | G, y) , \\ p(\tilde{y} = 1 | \tilde{G}, G, y) &= \int \sigma(\tilde{f}) p(\tilde{f} | G, y, \tilde{G}) d\tilde{f} , \end{aligned}$$

where

$$p(\tilde{f} | G, \tilde{G}, f) \sim N \left(k(\tilde{G})^T K^{-1} f, k(\tilde{G}) - k(\tilde{G})^T K^{-1} k(\tilde{G}) \right) .$$

Not surprisingly, our posterior is intractable, which means that our posterior predictive distributions are also intractable. In Section 3.1, we discuss implementation strategies including Markov chain Monte Carlo (MCMC) sampling and Monte Carlo integration.

It is worth noting a connection of our model with kernel SVM ([Rasmussen and Williams \(2005\)](#)). In GP classification, the log of the unnormalized posterior over the latent variables is

$$\log p(y|f) - \frac{1}{2} f^T K^{-1} f - \frac{1}{2} |K| - \frac{n}{2} \log 2\pi .$$

For a fixed kernel, the last two terms are constant, thus a GP classifier minimizes

$$(GPC) \quad \frac{1}{2} f^T K^{-1} f - \sum_{i=1}^n \underbrace{\log p(y_i|f_i)}_{\text{log likelihood}} .$$

On the other hand, kernel SVM minimizes

$$(SVM) \quad \frac{1}{2} f^T K^{-1} f - C \sum_{i=1}^n \underbrace{(1 - y_i f_i)_+}_{\text{hinge loss}} .$$

Based on the similarity of these objective functions, we expect the two methods to perform similarly for a fixed kernel, but of course the kernel hyperparameters are unknown. For the SVM, the cost penalty is also unknown. Besides the absence of a cost penalty, the GP classifier addresses this issue by placing priors over the kernel hyperparameters. In contrast, a grid search is typically used for an SVM, which is limiting unless the grid is chosen correctly. As we discussed in the introduction, this feature of GP classification directly follows from a Bayesian approach. Another consequence of the Bayesian approach is that we have proper probabilities associated with each prediction that come directly from our posterior. This allows us to perform uncertainty quantification for our predictions, as well as immediately yielding a technique for anomaly detection.

2.2. Anomaly Detection. One-class classification (OCC) is a classifier for a single class. For a review, see [Khan and Madden \(2009\)](#). Such a classifier is a type of anomaly detection that is useful when most of the data is from a single class and only a few, if any, training points are from another class.

The most common approach to OCC is through decision boundaries, which are typically found via SVMs. There are many variations of one-class SVM (OSVM) depending on the availability of training data, i.e whether any training data is from the negative class. Another approach to OCC is to simply use machine learning techniques for classification, like k-NN or tree-based methods, but these require negative training examples. However, neither OSVM nor non-OSVM solutions are probabilistic.

GP methods have been proposed as well for the OCC problem. [Kemmler et al. \(2013\)](#) suggests four GP values for OCC scores:

$$\begin{aligned} \tilde{\mu} &= \mathbb{E}[\tilde{f} | G, y, \tilde{G}] , & \tilde{\pi} &= p[\tilde{y} = 1 | G, y, \tilde{G}] = \sigma(\tilde{\mu}) , \\ \tilde{\sigma}^2 &= \text{Var}[\tilde{f} | G, y, \tilde{G}] , & \mathbf{H} &= \tilde{\mu} \cdot \tilde{\sigma}^{-1} . \end{aligned}$$

These values are obtained immediately from the posterior of our classification model. Unsurprisingly, [Kemmler et al. \(2013\)](#) notes that “tuning hyperparameters for one-classification tasks is a difficult task in a general setting without incorporating further model assumptions.” But this is exactly what we have accomplished by taking a Bayesian approach and putting priors over our kernel hyperparameters.

2.3. Survival Analysis. Fernández, Rivera and Teh (2016) introduce a semi-parametric Bayesian method for survival analysis that uses GPs to model variation around a parametric baseline hazard function. Their method easily incorporates covariates, censoring, and prior knowledge, while avoiding the proportional hazards constraint. By using our kernel inputs, we are able to adapt this model to perform survival analysis with network inputs.

Suppose we have data $(G_1, T_1), \dots, (G_N, T_N)$, where $G \in \mathcal{G}$ and T is a survival time on \mathbb{R}^+ with survival function S and hazard function λ . The authors model T as the first jump of a Poisson process with intensity λ . Together with the GP priors, the model for $T_i | G_i$ is

$$\begin{aligned} T_i | \lambda_i &\stackrel{ind}{\sim} \lambda(T_i) e^{-\int_0^{T_i} \lambda_i(s) ds} , \\ \lambda_i(t) | f, \lambda_0(t), G_i &= \lambda_0(t) \sigma(f(t, G_i)) , \\ f(\cdot) &\sim \mathcal{GP}(0, K) , \end{aligned}$$

where σ is the logistic function and K is a kernel in network and time. We take

$$(3) \quad K((t_1, G_1), (t_2, G_2)) = K_{\text{Ham}}(G_1, G_2) + K_T(t_1, t_2) ,$$

with K_T and K_{Ham} given in Equations (1) and (2), respectively, with shared signal variance σ^2 . The authors prove (*Proposition 1*) that for stationary kernels such as the squared-exponential, $S(t)$ associated with $f(t)$ is a proper survival function, i.e. for a fixed network G , we have $S_G(t) = \mathbb{P}(T > t | G) \rightarrow 0$ as $t \rightarrow \infty$.

Unfortunately, the likelihood for $T_i | G_i$ is (doubly) intractable since λ_i is defined by a GP. To overcome this, the authors develop a data augmentation scheme for sampling from an inhomogeneous Poisson process with intensity $\lambda_0(t)$, which allows a tractable reformulation of the model. Using the tractable model, which is a joint distribution on (R, T) , where R are (unknown) rejected jump points from a thinned Poisson process and T is the (known) first accepted one, the authors develop an inference algorithm that begins by sampling R . Crucially, the inference algorithm relies on sampling the GP f given $R \cup T$, which can be understood as GP binary classification. We provide implementation details in Section 3.2, including remarks on how our implementation differs from the original based on our use of network inputs.

3. Implementation. In this section, we provide implementation details for the models from Section 2. Full code is available at <https://github.com/KolaczykResearch/GP-Networks>.

3.1. Binary Classification and OCC. We develop a Gibbs sampler to overcome the intractability of our posterior. The posterior conditional distributions are as follows:

$$\begin{aligned} \sigma^2 | f, \ell &\sim \text{Inv-Gamma}\left(\alpha_\sigma + \frac{N}{2}, \beta_\sigma + \frac{f^T K_0^{-1} f}{2}\right) , \\ p(\ell | f, \sigma^2) &\propto \det(K)^{-1/2} e^{-\frac{1}{2} f^T K^{-1} f - \frac{\beta_\ell}{\ell}} \ell^{-\alpha_\ell - 1} , \\ p(f | \sigma^2, \ell) &\propto e^{-\frac{1}{2} f^T K^{-1} f} \prod_{i=1}^N \sigma(f_i y_i) . \end{aligned}$$

The signal variance parameter is conjugate, which makes sampling easy and in general this hyperparameter just controls the scaling of our latent function. However, the length scale parameters are coupled with the latent function, which makes sampling more challenging. Moreover, the determinant term adds unnecessary computational time if we elect to sample

f and ℓ separately. Instead, we sample them jointly following [Murray and Adams \(2010\)](#). Additionally, we make use of an elliptical slice sampler ([Murray, Adams and MacKay \(2010\)](#)) for better mixing of the latent function, which adds essentially no cost as the Cholesky is already cached. The pseudocode for our Gibbs sampler is given in Algorithm 1.

```

GPC Gibbs ( $K, Y, \alpha, \beta, ns$ );
Input : Kernel  $K$ , Labels  $Y \in \{\pm 1\}$ , inverse-gamma parameters  $\alpha$  &  $\beta$ , Number of samples  $ns$ 
Output: Posterior  $p(f|y, \theta)$ 
Initialize  $\sigma^2, \ell, f$ ;
for  $t = 2, \dots, ns$  do
    Jointly sample  $(f^{(t)}, \ell^{(t)}) \mid \sigma^{(t-1)}$  using slice sampler;
    Compute  $C_0$ , the Cholesky of  $K_0$  evaluated at  $\ell^{(t)}$ ;
     $C = C_0 \times \sqrt{\sigma^{(t-1)}}$ , the Cholesky of  $K$  evaluated at  $\sigma^{(t-1)}, \ell^{(t)}$ ;
    Sample  $f^{(t)} \mid \sigma^{(t-1)}, \ell^{(t)}$  cheaply using elliptical slice sampler;
    Sample  $\sigma_t^2 \sim \text{Inv-Gamma}\left(\alpha_\sigma + \frac{N}{2}, \beta_\sigma + \frac{f^T K_0^{-1} f}{2}\right)$ ;
     $C = C_0 \times \sqrt{\sigma^{(t)}}$ 
end

```

Algorithm 1: Gibbs algorithm for GP classification.

Note that the complexity of our sampler is dominated by the Cholesky decomposition of our kernel, which is a limitation inherent to GP methods. However, contrary to the claim in [Relión et al. \(2019\)](#), our method scales well in the size of the network, because a distance matrix D , with $D_{ij} = d_{\text{Ham}}(G_i, G_j)$, only needs to be computed once and can be done in parallel. Of course, other implementation strategies such as a grid search or maximizing the marginal likelihood would be faster than ours. However, these approaches lose the full benefit of a Bayesian framework, and in practice, we find they perform worse, as they are more limited in learning the kernel hyperparameters.

Suppose we have run Gibbs on a training set. To make predictions, first draw B samples from the posterior. Then, we can estimate f in two ways:

$$(4) \quad \hat{f} = \frac{1}{B} \sum_{b=1}^B k_{\theta^{(b)}}(\tilde{G})^T K_{\theta^{(b)}}^{-1} \hat{f} ,$$

$$(5) \quad \hat{f}_{\text{avg}} = k_{\hat{\theta}}(\tilde{G})^T K_{\hat{\theta}}^{-1} \hat{f} ,$$

where $\theta^{(b)}$ is the b^{th} sample of $\theta = (\sigma^2, \ell)$ and \hat{f} and $\hat{\theta}$ are the estimated posterior means of f and θ , respectively, all of which come from the Gibbs sampler. We recommend (4), which only requires one matrix inversion, as we see little difference in accuracy between the versions.

3.2. Survival Analysis. The posterior conditional distributions are as follows:

$$\begin{aligned} \sigma^2 \mid f, \ell_T, \ell_{\text{Ham}} &\sim \text{Inv-Gamma}\left(\alpha_\sigma + \frac{N + |R|}{2}, \beta_\sigma + \frac{f^T K_0^{-1} f}{2}\right) , \\ p(\ell_p \mid f, \sigma^2) &\propto \det(K)^{-1/2} e^{-\frac{1}{2} f^T K^{-1} f - \frac{\beta_p}{\ell_p}} \ell_p^{-\alpha_p - 1} , \\ p(f \mid \sigma^2, \ell) &\propto e^{-\frac{1}{2} f^T K^{-1} f} \prod_{i=1}^N \sigma(f(T_i)) \prod_{r \in R_i} (1 - \sigma(f(r))) . \end{aligned}$$

The pseudocode is given in Algorithm 2.

```

GP Survival ( $D, T, \alpha, \beta, ns$ );
Input : Distance array  $D$ , Survival times  $T$ , Hyperparameter priors  $\alpha$  &  $\beta$ , Number of samples  $ns$ 
Output: Samples from  $\lambda | T$ 
Initialize baseline hazard  $\lambda_0$  and kernel  $K$ ;
 $\lambda_0 = \Omega$  and  $\Lambda_0(t) = \Omega \cdot t$ ;
 $K_{ij} = \sigma^2 \left( \exp(-\ell_{\text{Ham}} \cdot D_{ij}^{\text{Ham}}) + \sum_{k=1}^p \exp(-\ell_k \cdot D_{ij}^p) + \exp(-\ell_T \cdot D_{ij}^T) \right)$ ;
Instantiate  $f$  in  $T$ ;
 $f^{(1)}(T) \sim \mathcal{N}(0, K)$ ;
for  $t = 2, \dots, ns$  do
  for  $i = 1, \dots, N$  do in parallel
     $n_i \sim \text{Poisson}(1; \Lambda_0(T_i))$ ;
     $\tilde{A}_i \sim \mathcal{U}(n_i; 0, \Lambda_0(T_i))$ ;
     $A_i = \Lambda_0^{-1}(\tilde{A}_i)$ ;
    Sample  $f(A_i) | f(R \cup T), \lambda_0$ ;
     $f^{(t)}(A_i) \sim \mathcal{N}(k(A_i, R \cup T)^T K^{-1} f^{(q-1)}(R \cup T), k(A_i, A_i) - k(A_i, R \cup T) K^{-1} K(R \cup T, A_i))$ ;
     $U_i \sim \mathcal{U}(n_i; 0, 1)$ ;
     $R_i = \{a \in A_i \text{ such that } U_i < 1 - \sigma(f(a))\}$ ;
  end
   $R = \bigcup_{i=1}^n R_i$ ;
  Update parameters of  $\lambda_0$ ;
   $\Omega \sim \Gamma(\alpha_\Omega + n + |R|, \beta_\Omega + \sum_{i=1}^n T_i)$ ;
  Update  $f(R \cup T)$  and hyperparameters of kernel as in Algorithm 1;
  Jointly sample  $f(R \cup T)$  and length scales for time and covariates using slice sampler;
  Sample  $f(R \cup T)$  several times using elliptical slice sampler;
  Sample signal variance from conjugate posterior;
end

```

Algorithm 2: Gibbs algorithm for GP survival analysis with constant baseline hazard function.

Note that f changes size at each iteration of the sampler: at $t = 1$, $R = \emptyset$ and $|f| = N$, whereas for $t \geq 2$, we have $|f| = N + |R|$. To update $f(R \cup T)$ in our slice sampler, we input the concatenation of $f(T)$ with $f(R)$, where the latter is from our previous sample $f(A)$. Also, notice that the sampling of rejected points and their imputation given $f(R \cup T)$ can be implemented in parallel, which was not discussed in the original paper. In addition, it is important to remember that each time point has associated covariates that are omitted in the notation, i.e. $f(t) = f(t, X)$, where X in this case is a network. Therefore, it is necessary to keep track of the implicit covariates when sampling A . Finally, as the authors point out, setting R can be seen as a GP classification problem. This procedures essentially uses a noisy version of our classifier from Section 2.1, which would be too computationally expensive to use at every step of the Markov chain.

We reiterate our advantage by using MCMC as there are many parameters crucial parameters to infer, including the baseline hazard rate and the multiple length scale parameters. On the other hand, this can be computationally slow if $|R|$ is large, which the authors circumvent using a kernel approximation. Unfortunately, such approximations are not available for network kernels because they rely on Bochner's theorem and Fourier transforms of kernels on \mathbb{R}^d .

Another computational note is that the kernels, while theoretically positive definite, can be numerically close to singular. For this reason, it is common to add jitter to the diagonal of

the kernel to improve the condition number. We find that more jitter is needed in the survival analysis setting than the binary classification, which is likely due to the fact that the rejected points R share all of the covariates with one of the original points, thereby introducing dependency into the rows and columns of the Gram matrix.

Having run the sampler, the survival surfaces are given as

$$S(t, X) = \exp \left(- \int_0^t \lambda(s, X) \, ds \right) .$$

We use the trapezoidal rule for integration by evaluating $f(s, X)$ on a uniform grid from $s = 0$ to $s = \max T$ with $\Delta = \frac{\max T}{99}$, i.e.

$$\int_0^t \lambda(s, X) \, ds \approx \frac{\Delta}{2} \sum_{k=1}^{100} \lambda(s_{k-1}, X) + \lambda(s_k, X) .$$

4. Theoretical Results. In this section, we define a graph distance and show that it induces a valid kernel. Using this kernel, we then prove that our binary classifier from Section 2.1 and our survival analysis from Section 2.3 both achieve posterior consistency.

4.1. PD Kernels. Central to the GP framework is a kernel for capturing the dissimilarity between data points. However, not all dissimilarity measures will induce a valid kernel, i.e a provably positive definite Gram matrix. This problem is further complicated by our use of network objects, as it is not obvious which graph distances will ensure a valid kernel.

While there are many known graph distance (Donnat et al. (2018)), we will work with the familiar Hamming distance. As it is commonly used, the Hamming distance is defined for two binary networks as the sum of the absolute differences of their corresponding adjacency matrices. However, as we will see in our proof of consistency, we need to work in the space of weighted networks. Moreover, we often encounter weighted networks, so using the edge weights rather than indicators for edges will provide us more information, and we can view binary networks as having weights in $\{0, 1\}$. In order to work with weighted networks, we must modify the Hamming distance slightly to guarantee its use in the squared-exponential kernel is valid.

DEFINITION 4.1. Let G_1 and G_2 be two simple networks over the same set of n vertices V with weighted adjacency matrices A and B , respectively. We define the weighted Hamming distance or Frobenius distance between G_1 and G_2 to be

$$d_{\text{Ham}}(G_1, G_2) := \frac{1}{n(n-1)} \sum_{i,j \in V} (A_{ij} - B_{ij})^2 .$$

THEOREM 4.2. If G_1, \dots, G_N are weighted networks and

$$K_{ij} = \sigma^2 \exp \left(-\ell \cdot d_{\text{Ham}}(G_i, G_j) \right) ,$$

then K is a positive-definite kernel.

PROOF. Jayasumana et al. (2013) provide the following theorem. Let (M, d) be a metric space and define $k : X \times X \rightarrow \mathbb{R}$ as $k(x_i, x_j) = \exp \{ -d^2(x_i, x_j)/2\sigma^2 \}$. Then k is positive definite for all $\sigma > 0$ if and only if there exists an inner product space V and a function

$\psi : M \rightarrow V$ such that $d(x_i, x_j) = \|\psi(x_i) - \psi(x_j)\|$. Using our weighted Hamming distance and absorbing the normalizing constant into σ^2 , we have

$$\begin{aligned} d_{\text{Ham}}(G_1, G_2) &= \sum_{i,j \in V} (A_{ij} - B_{ij})^2 \\ &= (A - B) \cdot (A - B) \\ &= \|A - B\|_{\text{F}}^2, \end{aligned}$$

where \cdot and $\|\cdot\|_{\text{F}}$ are the Frobenius inner product and norm, respectively. \square

Note that for binary networks, the sum of absolute differences is equal to the sum of squared differences, so our weighted Hamming distance is consistent with the commonly used Hamming distance for binary networks. It follows that Theorem 4.2 holds for binary networks and the usual Hamming distance.

4.2. Posterior Consistency of Classifier. Let G_1, \dots, G_N be simple weighted networks on the same set of n vertices, V . That is, $G_i = (V, E^{(i)}, W^{(i)})$ for all $i = 1, \dots, N$ with $w_{jj} = 0$ for all $j = 1, \dots, n$. Unlike many graph results that consider the asymptotic behavior as the order of the network, n , grows, we return to the classical data setting and investigate what happens as the sample size, N , of observed networks increases. With the set up from Section 2.1 with inverse-gamma hyperpriors over the kernel induced by our weighted Hamming distance, we show that our classifier achieves posterior consistency.

THEOREM 4.3. *GP classification with network inputs achieves posterior consistency for the squared-exponential kernel induced by our weighted Hamming distance.*

We defer the proof to the [Appendix](#). Ultimately, we show that our classifier achieves posterior consistency by verifying the conditions given in [Ghosal and Roy \(2006\)](#). Here, we make a few remarks about the proof.

First, the infinite differentiability of our kernel is important for verifying several of the conditions, which demonstrates the importance of using a squared-exponential kernel rather than, say, a Matérn kernel. This reiterates the need to have a graph distance that guarantees positive-definiteness of our squared-exponential kernel.

Secondly, it is important that we bound our covariate space, which forces us to work in the space of weighted networks. Again, this highlights the importance of our weighted Hamming distance to avoid the complexity of the space of binary networks.

Finally, the inverse-gamma hyperpriors ensure full support over the kernel hyperparameters. Although other fully supported priors could be used while maintaining posterior consistency, inverse-gamma is conjugate for the signal variance hyperparameter.

4.3. Posterior Consistency of Survival Analysis. As above, let G_1, \dots, G_N be simple weighted networks on the same set of vertices. Consider the survival analysis model from Section 2.3 with the kernel in network and time given by Equation (3). Under the assumption that the survival times have finite expectation, we show that our survival analysis model achieves posterior consistency in the limit of N .

THEOREM 4.4. *Under mild assumptions, survival analysis with network inputs achieves posterior consistency.*

Again, we defer the proof to the [Appendix](#), which consists of verifying the conditions given in [Fernández and Teh \(2016\)](#). The main assumption that we make is that the mean of the survival time is finite, which is true for events like death, and reasonable for many others. Otherwise, similar to Theorem 4.4, we rely on our use of a squared-exponential kernel, which is stationary with respect to our weighted Hamming distance.

5. Results. In this section, we validate our approach to binary classification, anomaly detection, and survival analysis in several simulated settings. After, we return to our motivating application of preterm delivery.

5.1. Simulations.

5.1.1. Binary Classification. Here, we present the results of a simulation study to assess the accuracy of our GP classifier. Our simulation is a fully crossed design varying the sample size ($N = 20, 60, 100$) and the network size ($n = 10, 50, 100$), as well as the random graph model from which we sample the network inputs. We compare Erdős-Rényi (ER) vs ER, stochastic block model (SBM) vs ER, and SBM vs SBM in three regime densities (low, medium, and high) totaling 81 comparisons. For instance, in the SBM vs ER medium regime, we sample

$$(6) \quad G \mid Y = -1 \sim \text{SBM} \begin{pmatrix} .55 & .45 \\ .45 & .55 \end{pmatrix} \quad \text{and} \quad G \mid Y = +1 \sim \text{ER}(.5) .$$

Every SBM has equal-sized communities and the edge probability of the ER model is equal to the average of the SBM within and between probabilities. When comparing ER vs ER and SBM vs SBM, the difference between expected network density is .1 for all three regimes.

For each network model, we sample $N/2$ networks and use a 75/25 train/test split to assess the classification accuracy. Results are given as the average accuracy over 100 replicates. The results also show a comparison to an SVM using the same squared-exponential kernel. For the SVM, we take the cost penalty $C = 1$, but perform 5-fold cross-validation for hyperparameter selection across a grid defined over 90% coverage of the same prior used for our GP classifier.

In 70% of simulations, our GP classifier outperforms the SVM, but in general they perform similarly, which is unsurprising considering the connection we made in Section 2.1 between the objective functions. Our GP classifier improves more as the sample size and network size increases, while for some simulations the SVM shows no improvement, for example in ER vs ER with medium density. The SVM had difficulty with both the SBM vs ER and the medium regimes, but excelled in the case of ER vs ER with either low or high density. We plot the results for SBM vs ER in Figure 4, while the remainder are available in the [Appendix](#).

Another observation is that the classification accuracy for our GP classifier has higher variance. This could be due to poor mixing, which was not evaluated for any of the simulations. Hand tuning, which is important for Bayesian modeling, is likely to further improve the results of the GP classifier, but is unrealistic in such a multifactorial simulation study. In addition, we only ran each chain for 2,500 samples, therefore dampening our advantage of sampling hyperparameter space over the grid search used by SVM.

While not a simulation, we also ran our classifier on the COBRE dataset from [Relión et al. \(2019\)](#). Using the same 10-fold cross-validation as reported by the authors, we obtained a mean AUC of .975 with a standard deviation of .047, which shows our GP classifier is capable of discriminating the two classes at a state-of-the-art level. Moreover, unlike the authors' methods, we do not use the test set to tune our hyperparameters. Furthermore, we do not require any preprocessing of the networks to select a subset of nodes and edges to be used.

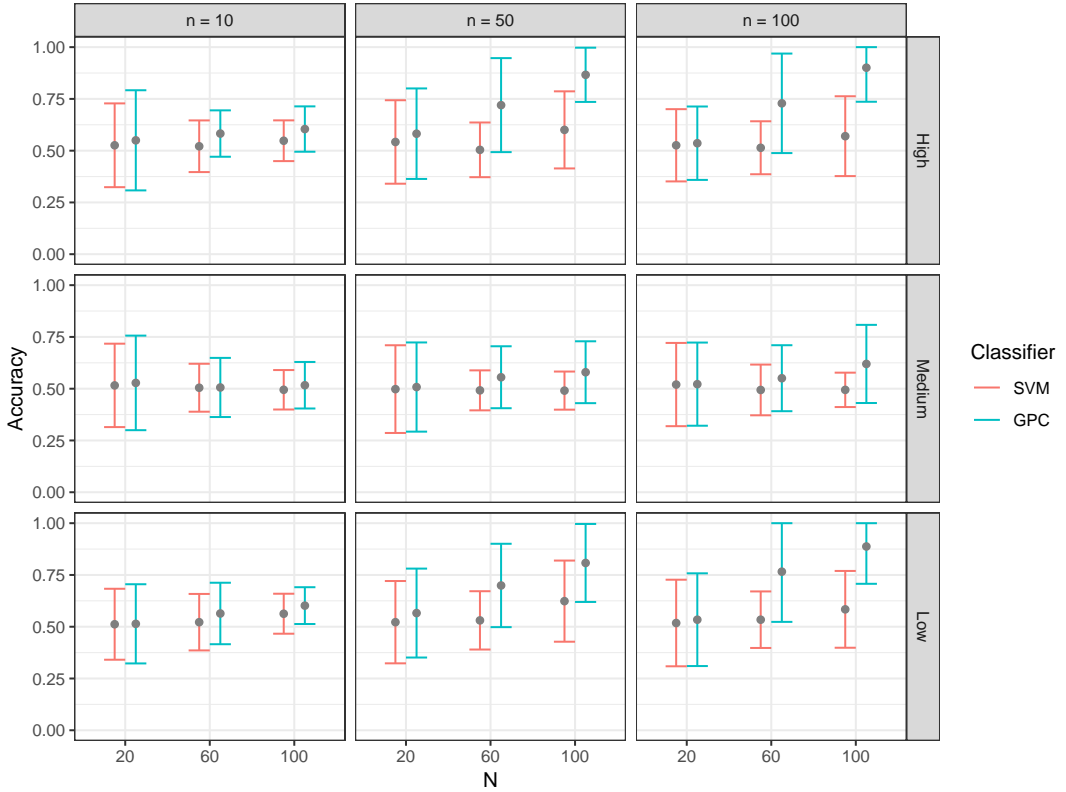


FIG 4. *Simulation results for all SBM vs ER settings. Simulations were repeated 100 times for each setting. The mean classification accuracy on the test set is shown along with one standard deviation.*

5.1.2. Anomaly Detection. Next, we emulate the scenario when one class is much more prevalent, yet we would like to be able to identify possible samples from another class perhaps as new samples become available. To do this, we consider a similar simulation as in Section 5.1.1, but train our classifier exclusively on one class. We set the classes as unbalanced, 90/10, but still use a 75/25 train/test split. For simplicity, we just consider (6) when $N = 100$ and $n = 50$, where the SBM is the more common class. From Figure 4, we see that this is one of the more difficult classification tasks for both our GP classifier and the SVM even when the classes are evenly balanced.

In this more challenging setting, unsurprisingly, our GP classifier predicts the single class for all of the new observations. Nevertheless, we see separation of the classes in Figure 5 for all of the OCC scores. This demonstrates the importance of a probabilistic model. That is, we can order test points by the likelihood of class membership and in this case, we are able to completely discriminate the test set even though all probabilities of belonging to the rare case are less than 0.5. Moreover, unlike other OCC methods that could be used to provide an ordering to test cases – for example, distance to decision boundary in OSVM – a fully probabilistic model provides multiple scores based on both first and second moments.

5.1.3. Survival Analysis. Finally, we consider two survival analysis problems. In the first case, we sample N points each from $f_0(t) = \mathcal{N}(2, 0.8^2)$ and $f_1(t) = \mathcal{N}(4, 1)$, restricted to \mathbb{R}^+ . However, instead of providing an indicator for which density a point was sampled from, we use as input a network sampled from $ER(p_0)$ or $ER(p_1)$. In this way, we simultaneously estimate the survival curves and perform classification. Moreover, we reduce to the noiseless

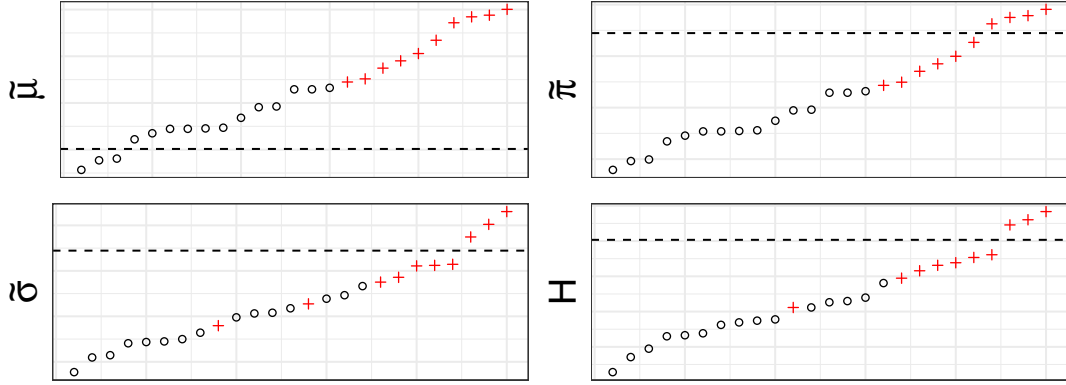


FIG 5. Four different OCC scores defined in Section 2.2 applied to our simulation test set. Scores are derived from the posterior of our GP classifier trained only on one class (black circle). Dashed lines indicate possible discrimination thresholds based on the elbow method, i.e. the largest jump among the sorted values.

case in the limit as $p_0 \rightarrow 0$ and $p_1 \rightarrow 1$. In the second case, we consider the more challenging variant from Fernández, Rivera and Teh (2016), in which $f_0(t) = \mathcal{N}(3, 0.8^2)$ and $f_1(t) = 0.4\mathcal{N}(4, 1) + 0.6\mathcal{N}(2, 0.8^2)$. This is similar to the first case except that $f_1(t)$ is now a mixture of the Gaussians in the first case, which creates a crossing between the survival functions corresponding to $f_0(t)$ and $f_1(t)$.

In both cases, we take $N = 50$ samples each from $f_0(t)$ and $f_1(t)$, where the network inputs are sampled from an *ER* with $n = 50$ nodes and $p_0 = .3$ and $p_1 = .7$. The results are shown in Figures 6 and 7. We see that we successfully estimate f_0 and f_1 in the easy case. On the other hand, the estimates in the hard case are essentially the mean of f_0 and f_1 , which are the same results as De Iorio et al. (2009), who originally introduced this experiment. Unfortunately, we would need a much larger N to recover the crossing survival functions, which is not feasible as our algorithm scales poorly in N even though parallelization helps. Although limiting, we note that our application only has a total of $N = 37$.

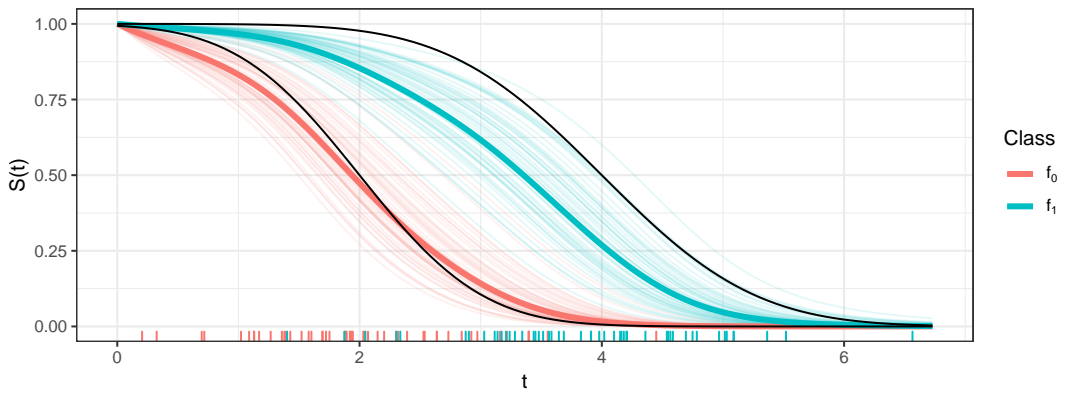


FIG 6. Simulation results for the easy case. The light curves are the posterior means of survival surfaces $S(t, G)$ for each point, the darker curves are survival curves $S(t)$ of each group, and the black curves are the true survival curves. We sample $N = 50$ points from each density and corresponding *ER* networks with $n = 50$ nodes with $p_0 = .3$ and $p_1 = .7$.

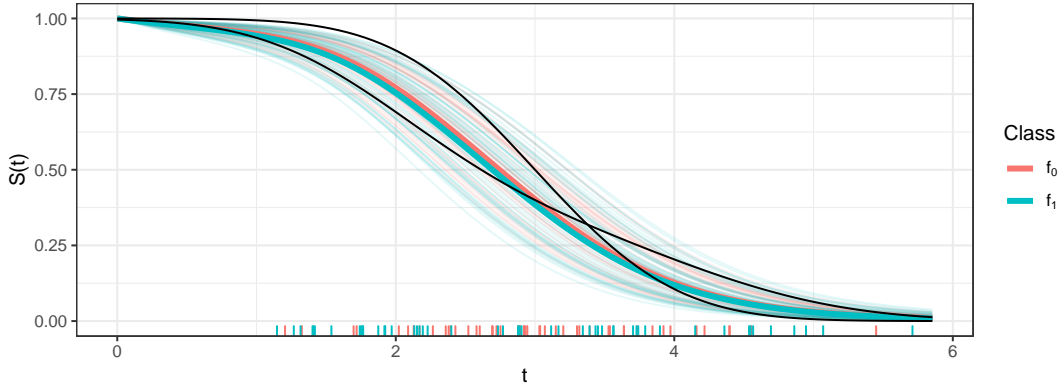


FIG 7. *Simulation results for the hard case.* The light curves are the posterior means of survival surfaces $S(t, G)$ for each point, the darker curves are survival curves $S(t)$ of each group, and the black curves are the true survival curves. We sample $N = 50$ points from each density and corresponding ER networks with $n = 50$ nodes with $p_0 = .3$ and $p_1 = .7$.

5.2. Microbiome Data. Finally, we return our attention to the microbiome dataset from [DiGiulio et al. \(2015\)](#). There are many methods for constructing microbiome networks using operational taxonomic unit (OTU) tables. We employ the SparCC method following [Friedman and Alm \(2012\)](#) and note that because we work in the space of weighted networks, we do not have to set arbitrary thresholds for assigning edges. However, we still need to make several preprocessing decisions on what samples to include. To do so, we follow similar guidelines as [Bogart, Creswell and Gerber \(2019\)](#), who use the same dataset, among others, to demonstrate their Bayesian method called MITRE for microbiome time-series data. In particular, we discard potentially spurious taxa with fewer than 500 total samples, exclude samples where coverage is lower than 1500 total samples, and restrict the samples to between 1 and 30 gestational weeks, but include samples from all body sites.

In addition to the microbial data, the dataset consists of clinical information including an indicator for a history of preterm delivery, an indicator if the given pregnancy resulted in a preterm birth, and the length of pregnancy. Using this data, we perform the following tasks. First, we define a classification problem using preterm delivery status. Note that [Bogart, Creswell and Gerber \(2019\)](#) perform the same classification task, but only group the preterm and very preterm labels in the dataset as preterm, whereas the original authors included the marginal label in the preterm class, which they define as before the 37th gestational week. In total, we have $N = 37$ networks with 11 preterm pregnancies, which is higher than the national average of 11% of pregnancies. For this reason, we also perform anomaly detection by only training on term pregnancies, which could be more relevant in practice. Finally, we perform survival analysis using days to delivery as our event.

Using leave-one-out cross validation (LOOCV), our classifier predicts term pregnancies for all but two of the subjects, which are both correctly predicted to be preterm. This is in contrast to the SVM, which predicts term for all subjects. This underscores the challenge of this classification task. However, LOOCV exacerbates the problem of unbalanced classes, since every time a subject with a preterm label is withheld, the classes become less balanced. For this reason, metrics like AUC are less useful. Instead, we reformulate the problem as an anomaly detection task by setting our training set to reflect the population, i.e. roughly 11% of training cases are preterm. We then run our GP classifier on this unbalanced training set to obtain OCC scores. The results of this are shown in Figure 8, which shows a low

false-positive rate for all the top-end scores, but nevertheless reiterates the challenge of this application. If microbiome sampling were to become part of prenatal care, then such scores could be used to flag high risk pregnancies.

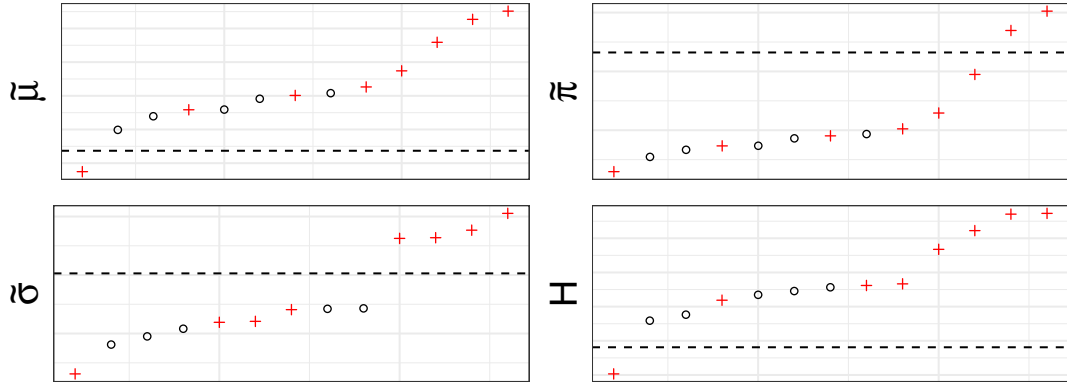


FIG 8. OCC scores for the microbiome data. Preterm births are denoted by a red plus sign and the dashed lines indicate the largest gap in values.

Finally, we perform survival analysis on time to birth, where we use as input both the subject's microbiome network and an indicator for history of preterm birth. Again, kernels provide an easy way to combine data of mixed types. The results are shown in Figure 9, which are compared against Kaplan-Meier (KM) estimates that only include the indicator as input.

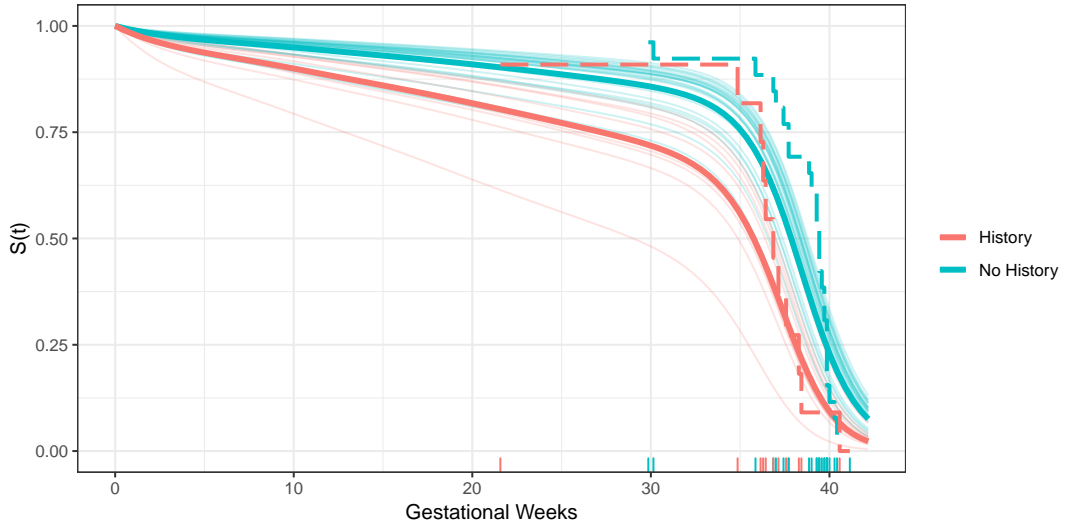


FIG 9. The light curves are the posterior means of survival surfaces $S(t, G)$ for each subject, the darker curves are survival curves $S(t)$ for those with and without history of preterm birth, and the dashed curves are Kaplan-Meier estimates.

One obvious difference between our GP method and the KM estimates is that smoothing allows us to extrapolate the likelihood of delivery prior to any observed time points. This extrapolation, however, retains the flexibility of the nonparametric KM method, while also incorporating relevant covariates such as the microbiome, which is known to effect gestational time. Ours is the only existing method that can incorporate these covariates as microbiome networks, which has become the standard tool for capturing the interconnectedness of the microbiome. Moreover, we are not beholden to strong assumptions such as proportional hazards as in the Cox model.

6. Conclusion.

6.1. Applications. In Section 5.2, we saw how our unified Bayesian framework for classification, anomaly detection, and survival analysis could be applied to a unique microbiome dataset. Originally, [DiGiulio et al. \(2015\)](#) demonstrated that microbiome networks captured the intricate dynamics between microbial taxa in pregnant women throughout gestation. Our work now represents an important advance in this research by providing statistical methodology for incorporating this data as network covariates. Consequently, we hope that this paper convinces practitioners across various scientific disciplines to collect network-based data objects and allows them to pose scientific questions using these networks as covariates. To the best of our knowledge, there are currently quite few datasets with individual networks and outcomes for all three problems of classification, anomaly detection, and survival analysis.

We believe that these tools will empower ecologists to design microbiome studies with many subjects across many time points, enabling further studies of relationships between the human microbiome and conditions such as pregnancy or various disease states. Additionally, these tools could be applied to a variety of non-human microbiomes and soil microbiomes, which are active areas of research.

Beyond ecology, our work is applicable to other fields that may benefit from the use of a network per individual or unit. As technological advances are making this increasingly possible, several areas in particular are poised to utilize these methods. For example, we have already shown that our models are useful in neuroscience for classifying diseases using fMRI networks. Furthermore, these methods can help address clinically relevant time-to-event questions about the brain such as the development of Alzheimer’s disease. Other areas of application include the detection of cancer using gene co-expression networks or single-cell networks, as well as social network analysis for identifying early adopters or performing time-to-purchase analyses using ego-nets.

6.2. Future Work. There are many exciting extensions to this work. First, it would be impactful if we had graph distances for networks of different orders, which would need to be induced by, or at the very least approximated by, inner products. For a recent review of graph distances, see [Donnat et al. \(2018\)](#). Next, we have seen that kernels seamlessly combine data of mixed types, such as patient networks and clinical information, but what about kernels that incorporate exogenous network information? Similarly, approximations of graph kernels in the spirit of [Rahimi and Recht \(2008\)](#) would speed up computations, and may be necessary as networks become more present and sample sizes increase. For survival analysis, it may be possible to adapt the recent variational approach by [Kim and Pavlovic \(2018\)](#) to network inputs. And, as always, we would benefit from better and faster MCMC or other Bayesian computational methods.

REFERENCES

BOGART, E., CRESWELL, R. and GERBER, G. K. (2019). MITRE: inferring features from microbiota time-series data linked to host status. *Genome biology* **20** 1–15.

BORGWARDT, K. M., ONG, C. S., SCHÖNAUER, S., VISHWANATHAN, S., SMOLA, A. J. and KRIEGEL, H.-P. (2005). Protein function prediction via graph kernels. *Bioinformatics* **21** i47–i56.

CORNEA, E., ZHU, H., KIM, P., IBRAHIM, J. G. and INITIATIVE, A. D. N. (2017). Regression models on Riemannian symmetric spaces. *Journal of the Royal Statistical Society: Series B (Statistical Methodology)* **79** 463–482.

DAI, X., MÜLLER, H.-G. et al. (2018). Principal component analysis for functional data on riemannian manifolds and spheres. *The Annals of Statistics* **46** 3334–3361.

DE IORIO, M., JOHNSON, W. O., MÜLLER, P. and ROSNER, G. L. (2009). Bayesian nonparametric nonproportional hazards survival modeling. *Biometrics* **65** 762–771.

DI GIULIO, D. B., CALLAHAN, B. J., McMURDIE, P. J., COSTELLO, E. K., LYELL, D. J., ROBACZEWSKA, A., SUN, C. L., GOLTSMAN, D. S., WONG, R. J., SHAW, G. et al. (2015). Temporal and spatial variation of the human microbiota during pregnancy. *Proceedings of the National Academy of Sciences* **112** 11060–11065.

DONNAT, C., HOLMES, S. et al. (2018). Tracking network dynamics: A survey using graph distances. *The Annals of Applied Statistics* **12** 971–1012.

DURANTE, D., DUNSON, D. B. and VOGELSTEIN, J. T. (2017). Nonparametric Bayes modeling of populations of networks. *Journal of the American Statistical Association* **112** 1516–1530.

FAUST, K., BAUCHINGER, F., LAROCHE, B., DE BUYL, S., LAHTI, L., WASHBURN, A. D., GONZE, D. and WIDDER, S. (2018). Signatures of ecological processes in microbial community time series. *Microbiome* **6** 120.

FERNÁNDEZ, T., RIVERA, N. and TEH, Y. W. (2016). Gaussian processes for survival analysis. In *Advances in Neural Information Processing Systems* 5021–5029.

FERNÁNDEZ, T. and TEH, Y. W. (2016). Posterior Consistency for a Non-parametric Survival Model under a Gaussian Process Prior. *arXiv preprint arXiv:1611.02335*.

FRIEDMAN, J. and ALM, E. J. (2012). Inferring correlation networks from genomic survey data. *PLoS computational biology* **8**.

GÄRTNER, T., DRIESSENS, K. and RAMON, J. (2003). Graph kernels and gaussian processes for relational reinforcement learning. In *International Conference on Inductive Logic Programming* 146–163. Springer.

GHOSAL, S. and ROY, A. (2006). Posterior consistency of Gaussian process prior for nonparametric binary regression. *The Annals of Statistics* **24** 13–249.

GINESTET, C. E., LI, J., BALACHANDRAN, P., ROSENBERG, S., KOLACZYK, E. D. et al. (2017). Hypothesis testing for network data in functional neuroimaging. *The Annals of Applied Statistics* **11** 725–750.

JAIN, B. J. (2016). On the geometry of graph spaces. *Discrete Applied Mathematics* **214** 126–144.

JAYASUMANA, S., HARTLEY, R., SALZMANN, M., LI, H. and HARANDI, M. (2013). Kernel methods on the Riemannian manifold of symmetric positive definite matrices. In *Computer Vision and Pattern Recognition (CVPR), 2013 IEEE Conference on* 73–80. IEEE.

KASHIMA, H. and INOKUCHI, A. (2002). Kernels for graph classification. In *ICDM workshop on active mining 2002*.

KEMMLER, M., RODNER, E., WACKER, E.-S. and DENZLER, J. (2013). One-class classification with Gaussian processes. *Pattern Recognition* **46** 3507–3518.

KHAN, S. S. and MADDEN, M. G. (2009). A survey of recent trends in one class classification. In *Irish conference on artificial intelligence and cognitive science* 188–197. Springer.

KIM, M. and PAVLOVIC, V. (2018). Variational Inference for Gaussian Process Models for Survival Analysis. In *UAI* 435–445.

KOLACZYK, E. D. and CSÁRDI, G. (2014). *Statistical analysis of network data with R* **65**. Springer.

KOLACZYK, E. D., LIN, L., ROSENBERG, S., WALTERS, J. and XU, J. (2020). Averages of unlabeled networks: Geometric characterization and asymptotic behavior. *The Annals of Statistics* **48** 514–538.

KONDOR, R. I. and LAFFERTY, J. (2002). Diffusion kernels on graphs and other discrete structures. In *Proceedings of the 19th international conference on machine learning* **2002** 315–322.

KRIEGE, N. M., JOHANSSON, F. D. and MORRIS, C. (2020). A survey on graph kernels. *Applied Network Science* **5** 1–42.

LAYEGHIFARD, M., HWANG, D. M. and GUTTMAN, D. S. (2017). Disentangling interactions in the microbiome: a network perspective. *Trends in microbiology* **25** 217–228.

MCNEISH, D. (2016). On using Bayesian methods to address small sample problems. *Structural Equation Modeling: A Multidisciplinary Journal* **23** 750–773.

MURRAY, I. and ADAMS, R. P. (2010). Slice sampling covariance hyperparameters of latent Gaussian models. In *Advances in neural information processing systems* 1732–1740.

MURRAY, I., ADAMS, R. P. and MACKAY, D. J. (2010). Elliptical slice sampling.

MYGDALIS, V., IOSIFIDIS, A., TEFAS, A. and PITAS, I. (2016). Graph embedded one-class classifiers for media data classification. *Pattern Recognition* **60** 585–595.

NIKOLENTZOS, G., SIGLIDIS, G. and VAZIRGIANNIS, M. (2019). Graph Kernels: A Survey. *arXiv preprint arXiv:1904.12218*.

PROCTOR, L. (2019). Priorities for the next 10 years of human microbiome research.

RAHIMI, A. and RECHT, B. (2008). Random features for large-scale kernel machines. In *Advances in neural information processing systems* 1177–1184.

RALAIVOLA, L., SWAMIDASS, S. J., SAIGO, H. and BALDI, P. (2005). Graph kernels for chemical informatics. *Neural networks* **18** 1093–1110.

RASMUSSEN, C. E. and WILLIAMS, C. K. I. (2005). *Gaussian Processes for Machine Learning (Adaptive Computation and Machine Learning)*. The MIT Press.

RELIÓN, J. D. A., KESSLER, D., LEVINA, E., TAYLOR, S. F. et al. (2019). Network classification with applications to brain connectomics. *The Annals of Applied Statistics* **13** 1648–1677.

RUDD, J. M. (2018). Application of support vector machine modeling and graph theory metrics for disease classification. *Model Assisted Statistics and Applications* **13** 341–349.

TANG, R., KETCHA, M., BADEA, A., CALABRESE, E. D., MARGULIES, D. S., VOGELSTEIN, J. T., PRIEBE, C. E. and SUSSMAN, D. L. (2018). Connectome smoothing via low-rank approximations. *IEEE transactions on medical imaging* **38** 1446–1456.

TOKDAR, S. T. and GHOSH, J. K. (2007). Posterior consistency of logistic Gaussian process priors in density estimation. *Journal of statistical planning and inference* **137** 34–42.

VISHWANATHAN, S. V. N., SCHRAUDOLPH, N. N., KONDOR, R. and BORGWARDT, K. M. (2010). Graph kernels. *Journal of Machine Learning Research* **11** 1201–1242.

ZHANG, W., OTA, T., SHRIDHAR, V., CHIEN, J., WU, B. and KUANG, R. (2013). Network-based survival analysis reveals subnetwork signatures for predicting outcomes of ovarian cancer treatment. *PLoS computational biology* **9** e1002975.

APPENDIX

PROOF OF THEOREM 4.3. Let $\varepsilon > 0$. We want to show that

$$\Pi\left(p : \int |p(x) - p_0(x)| dQ(x) > \varepsilon \mid Y_1, \dots, Y_N, X_1, \dots, X_N\right) \rightarrow 0 ,$$

which, by [Ghosal and Roy \(2006\)](#), happens just in case the following four conditions hold:

- (P) For every $x \in \mathcal{X}$, the covariance function $\sigma_0(x, \cdot)$ has continuous partial derivatives up to order $2\alpha + 2$, the mean function $\mu(x) \in \bar{\mathcal{A}}$, the RKHS of $\sigma_0(\cdot, \cdot)$, and the prior Π_λ is fully supported on $(0, \infty)$;
- (C) The covariate space \mathcal{X} is a bounded subset of \mathbb{R}^d ;
- (T) The transformed true response function $\eta_0 \in \bar{\mathcal{A}}$;
- (G) For every $b_1 > 0$ and $b_2 > 0$, there exist sequences M_n, τ_n and λ_n such that

$$M_N^2 \tau_N \lambda_N^{-2} \geq b_1 N \quad \text{and} \quad M_N^{d/\alpha} \leq b_2 N .$$

It is straightforward to verify conditions (P), (C), and (G):

- (P) The squared-exponential kernel is infinitely divisible, so we can take any $\alpha \in \mathbb{N}$ in (P). Furthermore, we are taking $\mu(x) = 0 \in \bar{\mathcal{A}}$ since all RKHS contain the identity element. Finally, we put an inverse-gamma prior on the bandwidth ℓ , which is fully supported on the positive reals;
- (C) The boundedness of our covariate space follows from the fact that we can embed the space of weighted networks in \mathbb{R}^{n^2} , where n is the number of nodes;
- (G) We can take $M_N = \ell_N$ and $\tau_N = b_1 N$. Then the result holds, since we can take any $\alpha \in \mathbb{N}$.

Note that the embedding of the space of weighted networks in \mathbb{R}^{n^2} is given by [Ginestet et al. \(2017\)](#).

Our only remaining obstacle to showing posterior consistency is (T). [Tokdar and Ghosh \(2007\)](#) provide an equivalency for (T). The authors show that

$$\eta_0 \in \bar{\mathcal{A}} \iff \forall \varepsilon > 0, \mathbb{P}(\|\eta(x) - \eta_0\|_\infty < \varepsilon) > 0$$

if the following three conditions hold:

- (A1) $\exists M, m > 0$ such that $m \leq \sigma_0(t, t) \leq M, \forall t \in (\mathbb{R}^+)^d$;
- (A2) $\exists C, q > 0$ such that $[\sigma_0(t, t) + \sigma_0(s, s) - 2\sigma_0(t, s)]^{1/2} \leq C\|s - t\|^q, \forall s, t \in (\mathbb{R}^+)^d$;
- (A3) For any $n \geq 1$ and any $t_1, \dots, t_n \in (\mathbb{R}^+)^d$, $\Sigma = ((\sigma(t_i, t_j)))$ is nonsingular.

First, we verify these conditions.

- (A1) Again, since we are using the squared-exponential kernel, for any distance $d(\cdot, \cdot)$, we have $d(t, t) = 0$ so that $\exp(-d^2(t, t)/2\sigma^2) = 1$. Therefore, take $m = 1 = M$;
- (A2) Since $\sigma_0(t, s) \leq 1$, we can take $q = 1$ to obtain

$$[1 + 1 - 2\sigma_0(t, s)]^{1/2} \leq \sqrt{2} .$$

Therefore, take $C = \sqrt{2}/\max_{s, t \in (\mathbb{R}^+)^d} |s - t|$;

- (A3) We already proved that the squared-exponential kernel induced by Hamming distance is positive-definite.

So, we are done if we can show

$$\forall \varepsilon > 0, \mathbb{P}(\|\eta(x) - \eta_0\|_\infty < \varepsilon) > 0 .$$

For $\varepsilon > 0$, we have

$$\begin{aligned}
\mathbb{P}(\|\eta(x) - \eta_0\|_\infty < \varepsilon) &\geq \mathbb{P}(\|\eta(x)\|_\infty + \|\eta_0\|_\infty < \varepsilon) = \mathbb{P}(\|\eta(x)\|_\infty < \varepsilon - |\eta_0|) \\
&= \mathbb{P}(\sup_x |\eta(x)| < \varepsilon - |\eta_0|) = 1 - \mathbb{P}(\sup_x |\eta(x)| > \varepsilon - |\eta_0|) \\
&\geq 1 - \exp(-(\varepsilon - |\eta_0|)^2/2) > 0 ,
\end{aligned}$$

where we used the Borell, or Borell-TIS, inequality in the fifth step, which says that for a mean-zero GP, X , with $\sigma^2(X) = \sup \text{Var}(X)$, we have

$$\mathbb{P}(\|X\|_\infty \geq x) \leq 2 \exp(-x^2/2\sigma^2(X)) .$$

Hence, $\eta_0 \in \bar{\mathcal{A}}$, verifying condition (T) and concluding our proof. \square

PROOF OF THEOREM 4.4. Fernández and Teh (2016) show that for a randomized design, the model for survival analysis in Section 2.3 occurs if the following four conditions hold:

- (A1) $(k(0) - k(2^{-n}))^{-1} \geq n^6$;
- (A2) ν assigns positive probability to every neighborhood of the true parameter;
- (A3) $\mathbb{E}_{\theta_0}[T] < M < \infty$;
- (A4) The true parameters $\eta_{j,0}$ take the form $\hat{\eta}_{i,0}/h_d$, where $\hat{\eta}_{i,0}$ is in the support of $\hat{\eta}_i$ under the uniform norm. $\hat{\eta}_j = h_d \eta_j$ is the non-stationary GP as a function of the original GP with

$$h_d(t) = \begin{cases} \frac{d+1}{1+\log(1-e^{-t})} & t < 1 \\ \frac{d+1}{t+\log(1-e^{-t})} & t \geq 1 \end{cases} .$$

The authors state that these assumptions are “quite reasonable and natural for the type of data we were dealing with.” In particular, we assume (A3) and (A4) hold. In words, (A3) just says that survival times have finite expectation, which is true for survival times like death. For others, like diagnosis, it is ill-posed to consider whether the likelihood goes to one as time increases. In general, this is a very reasonable assumption. On the other hand, (A4) is unverifiable, so we take it on faith.

For (A1), we note that for squared-exponential kernels, which is stationary, we have

$$k(s) = \sigma^2 \cdot \exp\left(-\frac{s^2}{2\ell^2}\right) = \sigma^2 \cdot \exp\left(-\tilde{\ell} \cdot s^2\right) ,$$

for some distance s . Hence, there is no ambiguity about what stationarity means for graph kernels, as the stationarity is with respect to, in our case, weighted Hamming distance. Therefore, we have

$$(k(0) - k(2^{-n}))^{-1} \geq n^6 \iff \frac{\left(1 - \exp\left(-\frac{\ell}{4r}\right)\right)^{-1}}{\sigma^2 \cdot n^6} \geq 1 .$$

This is true asymptotically, as the limit of the left side of the inequality goes to ∞ in n .

For (A2) We take a constant baseline hazard function $\lambda_0 = 2 \cdot \Omega$. This corresponds to a hazard function of an exponential random variable with mean $1/\Omega$, i.e. $\lambda_0 \sim \nu = \text{Exp}(\Omega)$, which is fully supported on the positive reals. \square

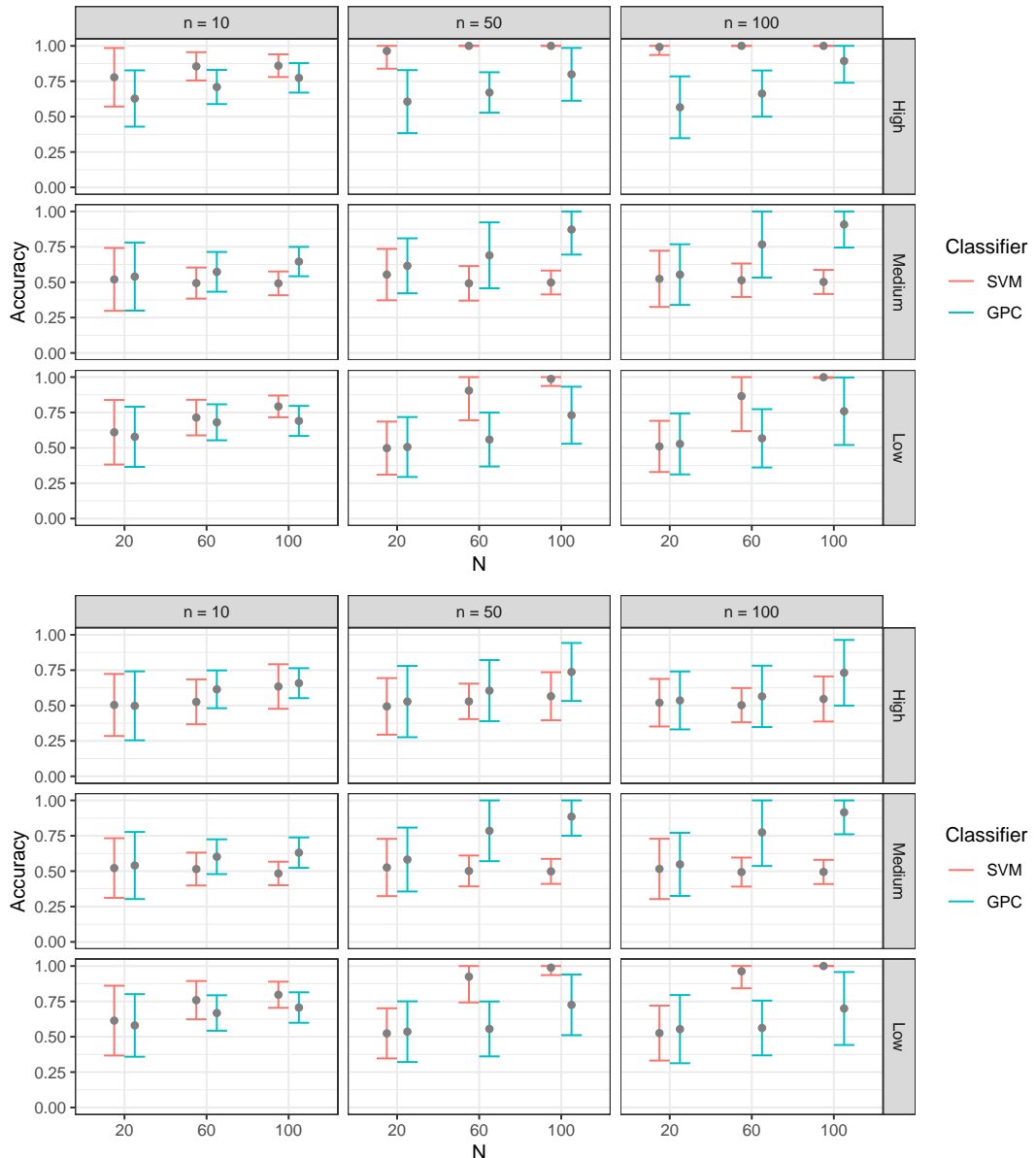


FIG 10. Remaining simulation results from Section 5.1.1. Top: ER vs ER. Bottom: SBM vs SBM. Simulations were repeated 100 times and one standard deviation is shown around the mean.